Proceedings of ITC18, 2008

Electron parallel heat transport in the scrape-off layer using a particle-in-cell code

Aaron FROESE[1)], Tomonori TAKIZUKA[2)] and Masatoshi YAGI[3)]

[1)]*IGSES, Kyushu University, Kasuga 816-8580, Japan*
[2)]*Japan Atomic Energy Agency, Naka 311-0193, Japan*
[3)]*RIAM, Kyushu University, Kasuga 816-8580, Japan*

Electron heat transport parallel to the magnetic field in the scrape-off layer plasma is investigated with the use of a particle-in-cell code PARASOL. Coulomb collisions are simulated correctly by a binary collision model. The heat flux is lost by radiation cooling, in addition to the convection/conduction to the divertor plates. It is confirmed for the collisional case that the conductive heat flux is given by the Spitzer-Härm expression. For the long mean free path case, the conductive heat flux is limited to a factor α_e of the free streaming value. It is found that α_e is small (~ 0.1 of the sheath-limited value) for the low radiation condition, but becomes large (~ 1.0) for the high radiation condition.

Keywords: tokamak scrape-off layer, conductive heat flux, PIC simulation, PARASOL, collisionless flux limit

1 Introduction

The divertor design in a tokamak reactor produces a separatrix system with closed magnetic field lines surrounded by open field lines terminating at the divertor plates. The burning core plasma lies inside the separatrix and exhibits good containment, though a large amount of heat is lost by anomalous transport and ELMs across the separatrix to the scrape-off layer (SOL). The heat in the SOL is carried mainly by the parallel transport along the open magnetic field lines to the divertor plates. Therefore, the SOL acts as a mediator between the hot core and the solid divertor plates.

Many features must be addressed in the SOL that are absent in the core; the plasma can no longer be assumed to be collisionless and strong parallel gradients develop that negatively affect the containment. In order to reduce the huge heat load on the plates, divertor simulation studies using fluid modelling are devoted to optimizing the divertor configuration and operation scenario. However, assumptions regarding kinetic effects, such as boundary conditions at the wall, heat conductivity, and plasma viscosity, are significant liabilities for the fluid model and are typically addressed by introducing primitive approximations [1, 2], which must be validated separately by full kinetic modelling. This can be accomplished by particle methods that suffer from large statistical errors or finite-difference methods that suffer from inefficient phase-space coverage. In this paper, electron heat transport parallel to the magnetic field in the SOL plasma is investigated with the use of a particle-in-cell code PARASOL in which Coulomb collisions are simulated correctly by a binary collision model.

author's e-mail: aaron@riam.kyushu-u.ac.jp

2 Parallel heat conduction

Parallel heat conduction by electrons is given by

$$q_e = \frac{m_e}{2} \int d\mathbf{v} \cdot V^2 V_{\parallel} f_e(\mathbf{x}, \mathbf{v}),$$

where m_e is the electron mass, $\mathbf{v}$ is the velocity, $\mathbf{V} = \mathbf{v} - \mathbf{u}$ is the velocity relative to the fluid velocity $\mathbf{u}$, and $f_e(\mathbf{x}, \mathbf{v})$ is the phase-space distribution function. In a collisional plasma, this evaluates to the Spitzer-Härm expression [3].

$$q_{SH} = -n_e \chi_e^{SH} \nabla_{\parallel} T_e \qquad \chi_e^{SH} = 3.2 v_{te} \lambda_{ee} \tag{1}$$

where n_e is the electron density, $v_{te} = (T_e/m_e)^{1/2}$ is the thermal speed, $\lambda_{ee} = v_{te}\tau_{ee}$ is the thermal mean free path, and $\tau_{ee} \propto v_{te}^3$ is the electron-electron collision time. Since χ has a strong dependence on thermal speed, which in turn depends on particle mass, so the ion conduction is negligible. However, this expression is not general due to the proportional relationship with the mean free path. The maximum heat flux in a collisionless plasma is the order of the free-streaming flux

$$q_{FS} = n_e T_e \left(T_{e\parallel}/m_e\right)^{1/2}. \tag{2}$$

We wish to determine the collision-dependent behavior of the heat flux, so as to replace it with a simpler expression that retains resonable accuracy. The preferred method is using the harmonic average form [1],

$$q_{eff} = \left(\frac{1}{q_{SH}} + \frac{1}{\alpha_e q_{FS}} \right)^{-1}, \quad \alpha_e = \lim_{\lambda_{ee} \to \infty} \frac{q}{q_{FS}}, \tag{3}$$

where α_e is the flux-limiting coefficient, *i.e.* the ratio between free-streaming and actual heat fluxes in the collisionless limit. Since the Spitzer-Härm heat flux is proportional to the mean free path, when the collisionality is high, $q_{SH} \ll \alpha_e q_{FS}$ becomes small and $q_e \simeq q_{SH}$, but when

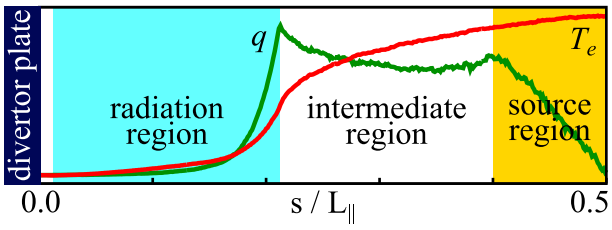

Fig. 1 Diagram of PARASOL half-system showing the temperature and heat flux profiles in the system with $f_{rad} = 0.5$ and $\lambda_{mfp}/L = 0.1$. The divertor plate (navy) and radiation (blue), intermediate (white), and source (yellow) regions are marked.

the collisionality is low, $q_{SH} \gg \alpha_e q_{FS}$ becomes large and $q_e \simeq \alpha_e q_{FS}$. A number of studies using kinetic simulations have produced widely disparate values for α_e, ranging from 0.03 to 3 [2]. However, there has been little inquiry into the cause of this range of results, with the exception of an investigation of the effect of collisionality using BIT1 [4]. In this study, we look at both collisionality as well as temperature gradient by adjusting the particle mean free path length and radiation loss from the SOL, respectively.

3 Simulation model

PARASOL is a 1d2v electrostatic particle-in-cell model on a closed domain with energy sources and sinks mirrored across the midpoint. The plasma is free to move in the spatial dimension s parallel to the separatrix magnetic field (Fig. 1a), but approximated as homogenous in the perpendicular directions. A hot ambipolar plasma source is in the domain center $s/L_{\|} = [0.4, 0.5]$ to mimic diffusion from the plasma core. Particles generated at the source are given a thermal velocity distribution consistent with the temperature of the particles already occupying the hot source region, essentially causing the core and SOL to equilibrate. Ions that strike the divertor plate are reintroduced as a hot ion-electron pair, maintaining a constant ion number in the simulation. Due to the fact that electrons escape sooner than ions, this leads to a slightly positive charge in the plasma.

Energy loss occurs via a radiative loss region and flow to the divertor plates. For this study, recycling at the divertor has been deactivated and neutrals are ignored. The divertor plate is set at an angle $\theta = 20°$ to the magnetic field, such that the connection length is related to the system length by $L = \theta L_{\|}$. The radiative energy sink lies beside the divertor $s/L_{\|} = [0.01, 0.21]$ to simulate radiation into the private plasma. During each time step, all electrons occupying the radiation region lose a small fraction of their kinetic energy with no change in direction. The input parameter $f_{rad} = Q_{rad}/Q_{tot}$ specifies the ratio of the radiative energy-loss flux to the total energy flux.

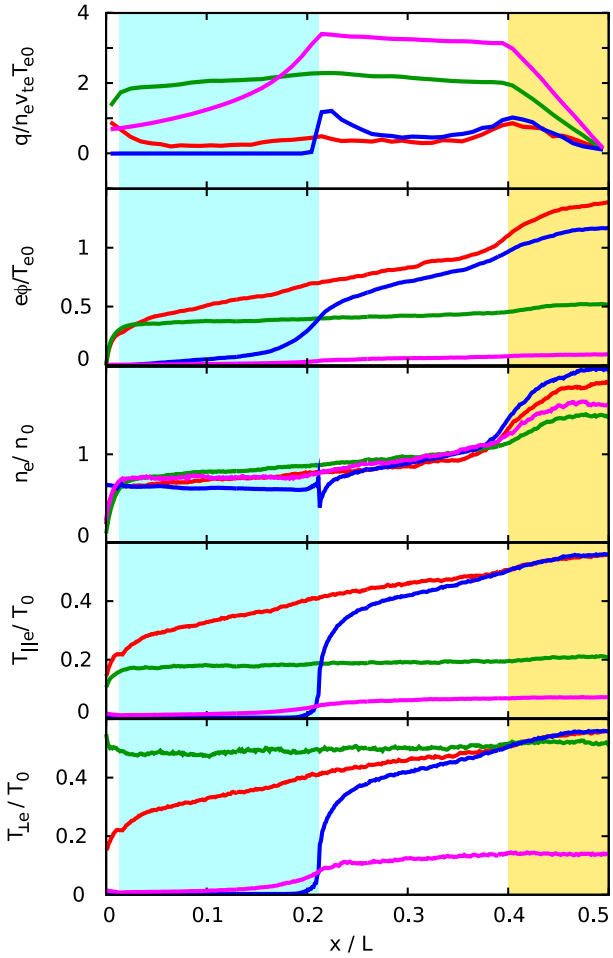

Fig. 2 Spatial variation profiles of conductive heat flux, potential, and electron density and temperature for plasma with the following properties:
(red) low rad. $f_{rad} = 0.1$, collisional $\lambda_{mfp}/L = 10^{-2}$
(green) low rad. $f_{rad} = 0.1$, collisionless $\lambda_{mfp}/L = 10^{2}$
(blue) high rad. $f_{rad} = 0.5$, collisional $\lambda_{mfp}/L = 10^{-1}$
(purple) high rad. $f_{rad} = 0.5$, collisionless $\lambda_{mfp}/L = 10^{3}$

Coulomb collisions are treated using a binary collision model, where in each time step each particle is paired with both an ion and another electron in the same cell, and given a collision angle proportional to the length of the time step. While the initial mean free path is specified as the input parameter $\lambda_{mfp0} \equiv 3^{3/2}\lambda_{ee}$, it evolves with the local plasma density and temperature such that $\lambda_{mfp}/\lambda_{mfp0} = (T_{e\|}/m_e)^{1/2}(3T_e/T_{e0})^{3/2}$. Ions progress in time via a kinetic equation and electrons by a drift kinetic equation. The ion gyro-radius is set to $\rho_i/L = 5\times10^{-3}$, the number of spatial cells to 800, and the number of particles per cell to greater than 100. Except where specified, the ion-electron mass ratio is always $m_i/m_e = 1800$.

4 Results

A cursory glance at the plasma profiles of high versus low collisionality and high versus low radiation rates shows

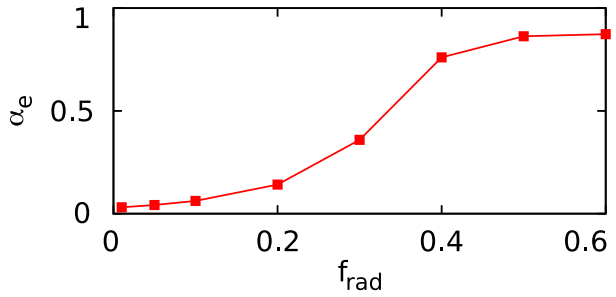

Fig. 3 Dependence of α_e in collisionless limit on radiation f_{rad}.

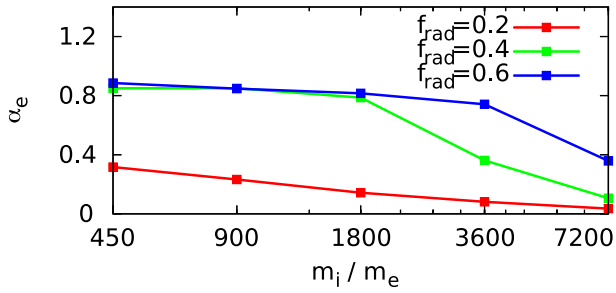

Fig. 4 Dependence of α_e in collisionless limit on ion-electron mass ratio m_i/m_e. Mass ratio 3600 corresponds to a deuterium plasma.

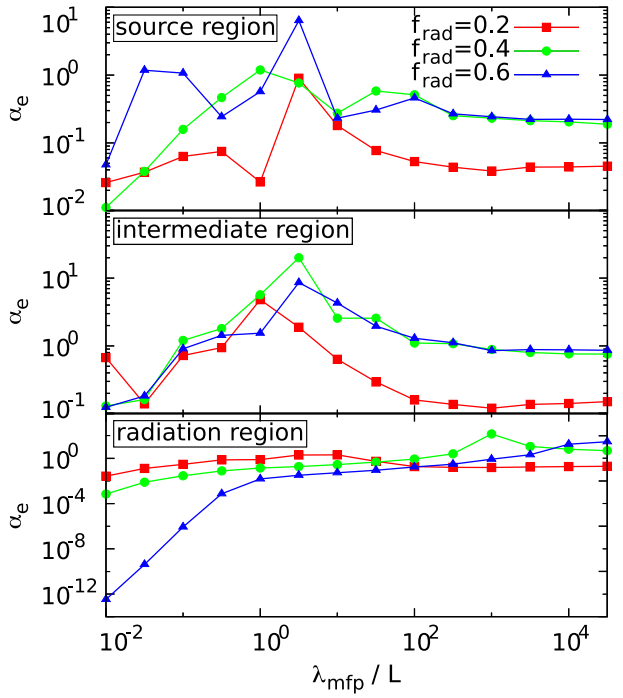

Fig. 5 Dependence of α_e on mean free path by region. Each point represents a poloidally-average over the indicated region with error bars omitted for clarity.

that the heat flux changes drastically in the four cases (Fig. 2). The collisional cases (red and blue) exhibit large gradients in potential, density and temperature compared to the collisionless cases (green and purple). They consequently have much smaller heat fluxes. As is expected, increasing the radiation causes the temperature and heat flux to drop precipitously before the divertor plate, but actually increases the rate of energy loss from the core plasma. In the collisional plasmas, the thermal energy is equally partitioned between all three dimensions, such that $T_{\|} = T_{\perp}$, whereas in the collisionless plasmas, the thermal energy is equally partitioned parallel and perpendicular to the magnetic field, such that $T_{\|} = T_{\perp}/2$.

The PARASOL code has previously been used to determine α_e to be a relatively high value of 0.75 for an ion electron mass ratio of $m_i/m_e = 400$ [5]. Our results show that this falls within the range of possible values seen in Fig. 4. The collisionless limit α_e has a simple harmonic form relationship with the radiation loss, growing from near zero when there is no radiation to nearly one when the energy reaching the divertor is negligible Fig. 3. The point of transition shifts to higher radiation as the mass ratio is increased, as Fig. 4 of ion-electron mass ratio dependence m_i/m_e shows. This shift occurs because high mass ions are less prone to collisional effects, spend less time in the radiation region, and therefore, the radiation becomes effectively less.

While α_e is defined as a collisionless limit without local energy sources or sinks, we wish to check if Eq. 3 can be used in the general case, as it often is. Therefore, the dependence of α_e on position and collisionality is of interest, with the results presented in Fig. 5. As expected, α_e always asymptotes to a constant value in the collisionless limit. This limit does not appear to depend on position (and hence energy balance) much, in keeping with the expectation that a sheath-limited plasma is almost uniform. The collisional limit, on the other hand, strongly changes with the local energy balance. In the source region, $q \simeq q_{SH}$, which results in large errors in the calculated value of α_e. The intermediate region shows a radiation-independent nearly linear growth with $\alpha_e \propto \lambda_{mfp}$ that results in a peak when the mean free path is on the order of the connection length. The radiation region exhibits similar linear growth, except that high radiation produces a much more rapid increase in α_e than low radiation.

We wish to examine the validity of using q_{eff} in Eq. 3 as a general substitute for the heat flux as calculated by a fully kinetic simulation. Figure 6 shows the relationship q/q_{eff} over a range of collisionalities and radiation rates. Of course, the function converges to unity at the collisionless limit because of the previous fitting to the free parameter α_e. However, without any fitting, the collisional limit also correctly shows that the heat flux approaches the Spitzer-Härm limit $q \rightarrow q_{SH}$. Unfortunately, as the function transitions from the Spitzer-Härm limit to the free-streaming limit, the simple model deviates from the actual heat flux. When the radiation rate is high, the match between q_{eff} and q is acceptably within error. However, as the radiation is reduced, such that particles become more likely to pass from the radiation region back into the inter-

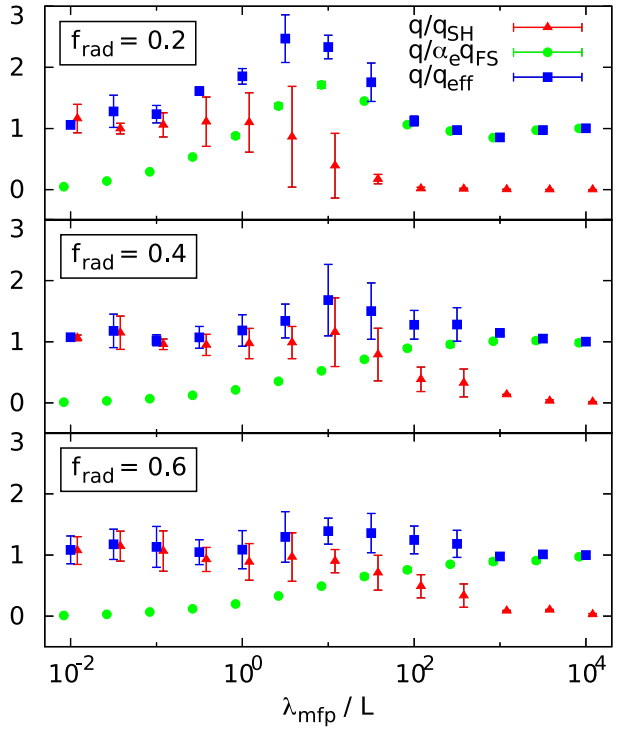

Fig. 6 Ratios of measured heat flux to Spitzer-Härm limit, α_e-adjusted free-streaming limit, and effective heat flux (Eq. 3) for different radiation rates and measured in the intermediate region. The values of α_e for each case are taken from the results in Fig. 6.

mediate region, the ratio $q/\alpha_e q_{FS}$ alone rises above unity for a moderate mean free path length. This result is due to both a rise in the heat flux, as well as a reduction in the free-streaming heat flux. This may be attributable to the fact that the temperature gradient falls drastically with collisionality in the high radiation case, but almost not at all in the low radiation case.

5 Summary

Electron heat transport parallel to the magnetic field in the SOL plasma is investigated with the PARASOL simulation. It is confirmed that in the collisional case the conductive heat flux is given by the Spitzer-Härm expression. In the collisionless case, conductive heat flux is limited to a factor α_e of the free-streaming value, with α_e small (~ 0.1 of the sheath-limited value) when little energy is lost to radiation, but becomes large (~ 1.0) when the radiation is high. Outside these limits, the currently used model of the conductive heat flux is an insufficient approximation for q_e. The model deviates strongly from the calculated results for a moderately collisional plasma with low radiation. Behavior in regions with energy sources or sinks also requires a multiply-defined α_e. Constraining usage of the model to regimes that behave correctly is not practical, and therefore, a more robust model is required. Due to the relative economy of system memory, a database lookup for q_e as a function of electron density and temperature may be the most tenable solution.

[1] P. C. Stangeby, *The Plasma Boundary of Magnetic Fusion Devices* (Taylor & Francis, New York, 2000) p. 660.
[2] W. Fundamenski, Plasma Phys. Control. Fusion **47**, R163 (2005).
[3] S. I. Braginskii, *Review of Plasma Physics Vol. 1, edited by M. A. Leontovich* (Consultants Bureau, New York, 1966) p. 205.
[4] D. Tskhakaya *et al.*, Contrib. Plasma Phys. **48**, 89 (2008).
[5] T. Takizuka *et al.*, Trans. of Fusion Technol. **39**, 111 (2001).